



Royal Netherlands Institute for Sea Research

This is a postprint of:

Meer, M.T.J. van der, Benthien, A., French, K.L., Epping, E., Zondervan, I., Reichart, G.-J., Bijma, J., Sinninghe Damsté, J.S., & Schouten, S. (2015). Large effect of irradiance on hydrogen isotope fractionation of alkenones in *Emiliana huxleyi*. *Geochimica et Cosmochimica Acta*, 160, 16-24

Published version: [dx.doi.org/10.1016/j.gca.2015.03.024](https://doi.org/10.1016/j.gca.2015.03.024)

Link NIOZ Repository: www.vliz.be/nl/imis?module=ref&refid=246034

[Article begins on next page]

The NIOZ Repository gives free access to the digital collection of the work of the Royal Netherlands Institute for Sea Research. This archive is managed according to the principles of the [Open Access Movement](#), and the [Open Archive Initiative](#). Each publication should be cited to its original source - please use the reference as presented.

When using parts of, or whole publications in your own work, permission from the author(s) or copyright holder(s) is always needed.

Large effect of irradiance on hydrogen isotope fractionation of alkenones in

***Emiliana huxleyi*.**

Marcel T.J. van der Meer^{1*}, Albert Benthien², Katherine L. French²⁺, Eric Epping¹,
Ingrid Zondervan², Gert-Jan Reichart^{1,3}, Jelle Bijma², Jaap S. Sinninghe Damsté^{1,3} and
Stefan Schouten^{1,3}

¹NIOZ Royal Netherlands Institute for Sea Research, PO Box 59, 1790 AB Den Burg,
The Netherlands (*corresponding author: Marcel.van.der.Meer@nioz.nl, Tel.:
+31222369568, Fax: +31222319674)

²Alfred-Wegener-Institute Helmholtz-Zentrum für Polar- und Meeresforschung, PO
Box 12 01 61, D-27515 Bremerhaven, Germany

³Faculty of Geosciences, Utrecht University, PO Box 80.021, 3508 TA Utrecht, The
Netherlands

⁺ Present day address: Woods Hole Oceanographic Institution, Cambridge, MA 02139,
United States

1 **Abstract**

2 The hydrogen isotopic (δD) composition of long-chain alkenones produced by
3 certain haptophyte algae has been suggested as a potential proxy for reconstructing
4 paleo sea surface salinity. However, environmental parameters other than salinity may
5 also affect the δD of alkenones. We investigated the impact of the level of irradiance on
6 hydrogen isotopic fractionation of alkenones versus growth water by cultivating two
7 strains of the cosmopolitan haptophyte *Emiliana huxleyi* at different light intensities.
8 The hydrogen isotope fractionation decreased by approximately 40‰ when irradiance
9 was increased from 15 to 200 $\mu\text{mol photons m}^{-2} \text{ s}^{-1}$ above which it was relatively
10 constant. The response is likely a direct effect of photosystem I and II activity as the
11 relationship of the fractionation factor α versus light intensity can be described by an
12 Eilers-Peters photosynthesis model. This irradiance effect is in agreement with
13 published δD data of alkenones derived from suspended particulate matter collected
14 from different depths in the photic zone of the Gulf of California and the eastern
15 tropical North Pacific. However, haptophyte algae tend to bloom at relatively high light
16 intensities ($> 500 \mu\text{mol photons m}^{-2} \text{ s}^{-1}$) occurring at the sea surface, at which hydrogen
17 isotope fractionation is relatively constant and not affected by changes in light intensity.
18 Alkenones accumulating in the sediment are likely mostly derived from these surface
19 water haptophyte blooms, when the largest amount of biomass is produced. Therefore,
20 the observed irradiance effect is unlikely to affect the applicability of the hydrogen
21 isotopic composition of sedimentary long chain alkenones as a proxy for paleosalinity.

22

23 **1. Introduction**

24 The oxygen and hydrogen isotopic composition of ocean water is strongly
25 correlated with salinity because phase changes between seawater, water vapor and
26 precipitation involves oxygen and hydrogen isotope fractionation. For instance, water
27 vapor is depleted in ^{18}O and D relative to water and evaporation thus results in increased
28 salinity and ^{18}O and D content of seawater in evaporative regions. The isotopically
29 depleted water vapor will condense and precipitate over continents and thus river runoff
30 and precipitation result in both a decrease in salinity and ^{18}O and D content of the
31 seawater. Therefore, for most parts of the ocean-atmosphere interface water isotopes are
32 linearly correlated with salinity (Craig and Gordon, 1965) and thus paleosalinity can be
33 reconstructed from either the oxygen or hydrogen isotopic composition of water using
34 this relation.

35 The hydrogen isotopic composition of water may be recorded in the non-
36 exchangeable hydrogen in biological organic matter although with a considerable
37 biosynthetic isotopic fractionation effect (Yakir and DeNiro, 1990; Hayes 2001).
38 Nevertheless, as long as this fractionation can be constrained, δD analyses on marine
39 organic matter could provide a means to reconstruct δD of seawater and, thus, if the
40 relation between δD and salinity is known, seawater paleosalinity. Long-chain
41 alkenones produced only by haptophyte algae such as *Emiliana huxleyi* (Volkman et
42 al., 1980; Marlowe et al., 1984; Volkman et al., 1995) possess only covalently bound
43 hydrogen atoms, which are not likely to be exchanged during diagenesis (Sessions et al.,
44 2004), making them excellent candidate compounds for stable hydrogen isotope
45 analysis. Initially the idea was to reconstruct paleo seawater δD directly from the
46 measured alkenone δD assuming a fixed difference between the alkenone and water
47 isotopic composition. This idea was motivated by the relatively constant fractionation of

48 approximately 225‰ between alkenones and water for batch cultures of the haptophyte
49 *Emiliania huxleyi* grown on medium spiked with different levels of deuterated water, at
50 constant salinities (Paul 2002; Englebrecht and Sachs 2005). However, experiments
51 with *E. huxleyi*, and other alkenone-producing haptophytes, i.e. *Gephyrocapsa*
52 *oceanica*, *Isochrysis galbana* and *Chrysotila Lamellosa*, cultured at different salinities
53 showed that the biological hydrogen isotope fractionation between alkenones and water,
54 expressed as the fractionation factor α , depends on salinity (Schouten et al., 2006;
55 M’Boule et al., 2014; Chivall et al., 2014). Therefore, as salinity increases not only the
56 hydrogen isotopic composition of water increases but α increases as well, both resulting
57 in an increased D content of alkenones with increasing salinity. This indicates the
58 potential of the δD of alkenones as a paleo sea surface salinity proxy. Several studies
59 indicate that salinity dependent hydrogen isotope fractionation might be a general
60 phenomenon in phototrophic organisms. For instance, hydrogen isotope fractionation in
61 cyanobacterial lipids from naturally occurring microbial mats decreases with increasing
62 salinity (Sachse et al., 2008) . The fractionation associated with dinosterol in the
63 Chesapeake Bay estuary (Sachs and Schwab, 2011) and dinosterol and brassicasterol
64 from saline and hypersaline lakes in North America (Nelson and Sachs, 2014) also
65 decreased with increasing salinity.

66 Consequently, the hydrogen isotopic composition of C_{37} alkenones has been
67 used to estimate paleo sea surface salinity (SSS) changes in the Aegean Sea at the time
68 of sapropel S5 deposition (van der Meer et al., 2007). Here the δD record of combined
69 C_{37} alkenones ($C_{37:2}$ and $C_{37:3}$) showed a large and abrupt shift to lower δD values at the
70 onset of sapropel deposition similar to the shift observed for foraminiferal $\delta^{18}O$ values
71 measured on the carbonate tests of surface dwelling foraminifera (Marino et al., 2007).

72 This shift towards more D depleted alkenones suggests that this proxy does indeed
73 record the drop in SSS caused by the significantly increased input of freshwater from
74 the continent at the onset of sapropel formation. The δD alkenone proxy has
75 subsequently been used to assess paleo SSS changes in the Black Sea (van der Meer et
76 al., 2008; Giosan et al., 2012; Coolen et al., 2013) and glacial-interglacial salinity
77 changes in the Agulhas leakage area (Kasper et al., 2014) and Mozambique channel
78 (Kasper et al., 2015).

79 Despite these successful applications of the δD alkenone proxy for the
80 reconstruction of paleo SSS, several complications exist. Firstly, the δD of alkenones in
81 the Chesapeake Bay estuary and from saline and hypersaline lakes in continental North
82 America shows a correlation with the δD of the water, but does not reveal a relation of
83 the fractionation factor α between alkenones and growth water with salinity as observed
84 in for cultures (Schwab and Sachs, 2011; Nelson and Sachs, 2014). Secondly, factors
85 other than salinity have been shown to also affect the fractionation factor α between
86 alkenones and growth water. For example, *E. huxleyi*, *G. oceanica*, *I. galbana* and *C.*
87 *lamellosa* all show differences in α at the same salinity (Schouten et al., 2006; M'Boule
88 et al., 2014; Chivall et al., 2014) and the relationships between α and salinity are
89 different for cultures harvested during different growth phases (Wolhowe et al., 2009;
90 Chivall et al., 2014). Additionally, it has been suggested that growth rate also affects α
91 (Schouten et al., 2006). A yet unexplored factor in determining hydrogen isotope
92 fractionation is light intensity, which might have an effect because the production of
93 NADPH, the major source of hydrogen in biosynthesis (Zhang et al., 2009), is directly
94 linked to photosynthetic activity (Allen 2002). Here, we examined the impact of

95 irradiance on the hydrogen isotope fractionation in *E. huxleyi* and discuss the
96 implication of our findings for hydrogen isotopic fractionation in natural settings.

97

98 **2. Materials and methods**

99 *2.1 Incubation experiments*

100 Two sets of light experiments were carried out. Monospecific cultures of the
101 haptophyte algae *E. huxleyi* (strain PML B92/11) were grown at a constant temperature
102 of 15°C, at a constant salinity of 32.5, and varying light intensities of 15, 30, 50, 100
103 and 200 $\mu\text{mol photons m}^{-2} \text{ s}^{-1}$. In a second experiment, batch cultures of *E. huxleyi*
104 (strain RCC1238) were grown in triplicate at four different light intensities (100, 200,
105 400, and 600 $\mu\text{mol photons m}^{-2} \text{ s}^{-1}$) in autoclaved 1 L bottles at a constant temperature
106 and salinity of 15°C and 32.2, respectively. The two strains show similar growth
107 responses relative to nutrients, temperature, light etc. The main difference between the
108 two strains has to do with differences in their carbonate chemistry (Langer et al., 2009).
109 All cultures were grown in Rumed cabinets, providing cool-white fluorescent light with
110 a 16:8 h light:dark cycle. The seawater medium prepared according to F/2 (Guillard,
111 1975) for the first and F/2R for the second experiment, respectively. The enriched
112 medium was sterile filtered using a 0.45 μm filter cartridge in the first experiment and
113 0.2 μm filter cartridge in the second experiment. All cultures were allowed to acclimate
114 to the experimental conditions in a pre-culture before being used to inoculate the main
115 batch cultures to provide an initial cell density between $0.5\text{-}7\times 10^3 \text{ cell ml}^{-1}$ for the first
116 experiment and a target initial cell density of approximately $0.9\times 10^2 \text{ cell ml}^{-1}$ for the
117 second experiment. Cultivation took place in bottles that were closed and incubated for
118 4 to 12 days depending on algal growth rate.

119 Cells were counted daily using a Beckman Coulter Multisizer 3 particle counter.
120 Cell numbers were log transformed and plotted versus time, growth rate μ (d^{-1}) was
121 estimated by linear regression. The cultures were harvested by filtration over ashed 0.7
122 μm GF/F filters (Whatman) when the cultures were in exponential growth phase and
123 had achieved cell densities within the range of $0.55-1.5 \times 10^5$ cells ml^{-1} . Filters and
124 aliquots of the culture medium were frozen immediately and stored at $< -25^\circ C$ until
125 analysis. The culture waters were stored with no headspace in 12 mL exetainers (Labco)
126 in the dark at $\sim 5^\circ C$ until analysis.

127

128 *2.2 Alkenone preparation*

129 Filters from the first experiment were extracted ultrasonically using first
130 methanol, followed by methanol:dichloromethane (DCM) 1:1 (v:v) and finally DCM. A
131 ketone fraction was obtained by purifying the total lipid extracts by passing them over a
132 silica gel cartridge (Varian Bond Elut; $1\text{ cm}^3/100\text{ mg}$), followed by saponification in 0.3
133 mL of 0.1 M KOH in methanol : water 9:1 (v/v) at $80^\circ C$ in a capped vial for 2 hours.
134 The alkenone containing fraction was subsequently obtained by partitioning in hexane
135 (Benthien et al., 2002). The alkenone fractions were analyzed by gas chromatography
136 (GC) and GC/mass spectrometry (GC/MS) (van der Meer et al., 2007). The alkenone
137 hydrogen isotopic composition was determined by GC thermal conversion isotope ratio
138 monitoring MS (GC/TC/irMS).

139 Filters from the second experiment were freeze dried for 24 h prior to automated
140 solvent extraction by a Dionex ASE using a 9:1 (v:v) DCM:methanol mixture. Total
141 lipid extracts (TLEs) were dried down using a rotary evaporator. The TLEs were
142 subsequently saponified by adding methanol and 1 ml 0.1 M KOH and heating at $80^\circ C$

143 for 2 h. The saponified alkenone fraction was analyzed by gas chromatography with
144 flame ionization detection (GC-FID).

145

146 *2.3 Instrumental analysis*

147 The algal culture media δD water values were determined by Elemental Analysis
148 (EA)/Thermal Conversion (TC)/irmMS using a Thermo Electron EA/TC coupled to a
149 Thermo Electron DELTA^{Plus} XL mass spectrometer for the first experiment according to
150 Schouten et al., 2006. In short, about 1 μ l of water was injected into a glassy carbon
151 filled ceramic tube at a temperature of 1425 °C. The H_3^+ -factor was determined daily
152 and was approximately 8.0 ± 0.3 ppm mV^{-1} . Waters were analyzed with at least ten
153 replicate analyses. Hydrogen gas with a predetermined isotopic composition was used
154 as reference and the water isotope values were calibrated against in-house lab standards
155 (North Sea water: +5‰ and bidistilled water: -76‰ that were calibrated by using
156 Vienna Standard Mean Ocean Water (VSMOW) and Greenland Ice Sheet Precipitation
157 (GISP) standards). The hydrogen isotopic composition of the medium used in the
158 second experiment was determined by the hydrogen gas-water equilibrium method
159 using a gas bench coupled to a Thermo Electron DELTA^{Plus} XP (Wong and Clarke,
160 2012) at the University of Utrecht.

161 Compound-specific hydrogen isotopic compositions for the combined C_{37}
162 alkenones (cf. van der Meer et al., 2013) from the first experiment were measured by
163 GC/TC/irmMS using a Thermo Electron DELTA^{Plus} XL mass spectrometer using a
164 CPSil 5 GC column with a 0.4 μ m film thickness and a constant flow of He of 1 ml
165 min^{-1} . Compounds were converted to hydrogen gas and graphite at 1425 °C in an empty
166 ceramic tube which was pre-conditioned by injecting 0.2 μ l of hexane several times (~5)

167 in the first week after installing a new reactor tube. Hydrogen gas with a predetermined
168 isotopic composition was used as reference gas at the beginning and end of each
169 analytical run and a C₁₆-C₃₂ *n*-alkanes mixture with offline determined isotopic
170 compositions (ranging from -42‰ to -256‰ vs. VSMOW, Schimmelmann MixB)
171 was used to monitor the system performance daily. The average offsets between the
172 measured δD values of the C₁₆-C₃₂ *n*-alkanes and their offline determined values were
173 generally 5‰ or less. Samples were analyzed at least in duplicate and the
174 reproducibility was typically better than 5‰ (Table 1). As additional control, squalane
175 was co-injected with every analysis and the average squalane value typically was -166 ±
176 3 ‰, while the offline determined value was -170‰.

177 Compound-specific hydrogen isotope values for the alkenones from the second
178 experiment were determined by GC/TC/irmMS with a Thermo Electron DELTA^{Plus} XP
179 mass spectrometer using high temperature conversion at the University of Utrecht.
180 Compounds were converted to hydrogen gas and graphite in an empty ceramic tube
181 heated to 1400 °C. The hydrogen isotopic composition of the combined C₃₇ alkenones
182 was corrected using the Schimmelmann *n*-alkane mix, Mix A. A squalane standard was
183 co-injected with every sample and its average value was -166.3 ± 5.1 ‰, which
184 compared well with its offline determined value of -169‰.

185

186 *2.4 Modelling*

187 A modified Eilers-Peeters formulation (Eilers and Peeters, 1988) was used to
188 describe both growth rate μ and fractionation factor α in response to irradiance. This
189 model can be applied directly to describe growth rate μ :

$$\mu = \mu_{max} * \frac{2 * (1 + \beta) * I/I_{opt}}{\left(I/I_{opt}\right)^2 + 2 * \beta * I/I_{opt} + 1} \quad (Eq. 1)$$

190 where β is a shape factor and μ_{max} represents the maximum growth rate. Growth rate μ
 191 attains a maximum value at optimal irradiance (I_{opt}). The shape factor β determines the
 192 'peakedness' or rounding of the production curve (e.g. Soetaert et al., 1994).

193 The model cannot be applied directly to describe hydrogen isotope fractionation,
 194 as the α value does not equal zero in the dark. Therefore the basic equation was
 195 extended with an offset value, α_0 , which defines the fractionation at zero light intensity:

$$\alpha = \alpha_0 + \gamma * \frac{2 * (1 + \beta) * I/I_{opt}}{\left(I/I_{opt}\right)^2 + 2 * \beta * I/I_{opt} + 1} \quad (Eq. 2)$$

196 where α attains a maximum value at I_{opt} equal to $\alpha_{max} = \alpha_0 + \gamma$. Parameter values
 197 μ_{max} , α_0 , α_{max} , and I_{opt} were estimated by minimizing the sum of squared differences
 198 between the model and experimental data using the Excel Solver routine.

199

200 3. Results

201 We analyzed the δD values of alkenones produced by *E. huxleyi* grown in batch
 202 cultures at different irradiance levels. For the first experiment, where *E. huxleyi* strain
 203 PML B92/11 was grown with light intensities ranging from 15 to 200 $\mu\text{mol photons m}^{-2}$
 204 s^{-1} , the relationship between the growth rate and irradiance indicates that *E. huxleyi* is
 205 growing under light limitation at light intensities $< 100 \mu\text{mol photons m}^{-2} \text{s}^{-1}$. Growth
 206 rate is approximately 0.5 d^{-1} at the lowest irradiance and increases to approximately 1.0
 207 d^{-1} at $50 \mu\text{mol photons m}^{-2} \text{s}^{-1}$. The growth rates level off at approximately 1.1 d^{-1} for
 208 irradiances exceeding $100 \mu\text{mol photons m}^{-2} \text{s}^{-1}$ (Table 1; Fig. 1). For the second
 209 experiment with *E. huxleyi* strain RCC1238 and irradiance levels ranging from 100 to

210 600 $\mu\text{mol photons m}^{-2} \text{ s}^{-1}$, a relatively constant growth rate of approximately 1.3 d^{-1} was
211 observed (Table 1; Fig. 1). The growth rates for *E. huxleyi* strain RCC1238 in
212 experiment 2 are slightly higher than for strain PML B92/11 in experiment 1 at the
213 corresponding irradiances of 100 and 200 $\mu\text{mol photons m}^{-2} \text{ s}^{-1}$.

214 The hydrogen isotopic composition of the combined $\text{C}_{37:2}$ and $\text{C}_{37:3}$ alkenones
215 ranged from approximately -230 ‰ at the lowest level of irradiance to
216 approximately -189 ‰ at an irradiance of 200 $\mu\text{mol photons m}^{-2} \text{ s}^{-1}$ for the first
217 experiment (Table 1). For the second experiment the isotopic composition of the
218 combined $\text{C}_{37:2}$ and $\text{C}_{37:3}$ alkenones ranged from approximately -212 ‰ at 100 μmol
219 $\text{photons m}^{-2} \text{ s}^{-1}$ to -188 ‰ at 200 $\mu\text{mol photons m}^{-2} \text{ s}^{-1}$. At irradiance levels $> 200 \mu\text{mol}$
220 $\text{photons m}^{-2} \text{ s}^{-1}$ the δD alkenones was approximately -193 ‰ .

221 The fractionation factor α between the hydrogen isotopic composition of the
222 alkenones and the culture medium ranged from approximately 0.77 at the lowest level
223 of irradiance to approximately 0.82 at an irradiance $>200 \mu\text{mol photons m}^{-2} \text{ s}^{-1}$ (Table
224 1). A strong and positive linear relationship between the fractionation factor α and
225 irradiance is observed for the first set of experiments up to an irradiance level of 200
226 $\mu\text{mol photons m}^{-2} \text{ s}^{-1}$ (Fig. 2). For the second experiment, the fractionation factor shows
227 values similar to those of experiment 1 at corresponding irradiance levels of 100 and
228 200 $\mu\text{mol photons m}^{-2} \text{ s}^{-1}$ (Fig. 2). This suggests that the two strains fractionate similarly
229 at similar irradiance levels. At light intensities exceeding 200 $\mu\text{mol photons m}^{-2} \text{ s}^{-1}$ α
230 decreases slightly from approximately 0.815 to approximately 0.805 (Table 1).

231

232 4. Discussion

233 4.1 Influence of the level of irradiance on the hydrogen isotopic fractionation.

234 Our culture results demonstrate that the level of irradiance affects both the growth
235 rate of *E. huxleyi* (Fig. 1) and the hydrogen isotope fractionation between the alkenones
236 produced and the water (Fig. 2). The growth rate increased linearly with irradiance up to
237 between 50 and 100 $\mu\text{mol photons m}^{-2} \text{ s}^{-1}$, and leveled off at irradiances above 100
238 $\mu\text{mol photons m}^{-2} \text{ s}^{-1}$. Even though the data are from experiments using two different *E.*
239 *huxleyi* strains, the combined data of growth rates versus irradiance can be described by
240 a single fit with the Eilers-Peeters model (Eq. 1) ($R^2 = 0.89$; Fig. 1). Based on these
241 results, it seems growth of *E. huxleyi* is not inhibited by irradiance levels of up to 600
242 $\mu\text{mol photons m}^{-2} \text{ s}^{-1}$.

243 The decrease in α at higher irradiance levels ($> 200 \mu\text{mol photons m}^{-2} \text{ s}^{-1}$; Fig. 2) is
244 similar to what is typically observed in Photosynthesis-Irradiance curves and is typically
245 attributed to light inhibition (e.g. Eilers and Peeters, 1988). A modified Eilers-Peeters
246 type of equation (Eq. 2) was used to describe the observed relationship of irradiance
247 with α , yielding a good fit ($R^2 = 0.94$; Fig. 2). This fit predicts a maximum fractionation
248 factor of 0.814 at an optimum irradiance (I_{opt}) of approximately 310 $\mu\text{mol photons m}^{-2} \text{ s}^{-1}$,
249 which is in the range of saturation irradiance (I_{sat}) values (200-400 $\mu\text{mol photons m}^{-2}$
250 s^{-1}) reported for photosynthesis in *E. huxleyi* strains (Flameling and Kromkamp, 1998;
251 Feng et al., 2008; Harris et al., 2005). However, higher and lower I_{sat} values have also
252 been reported (Nanninga and Tyrrell 1996, and references therein). Because the
253 modified Eilers-Peeters equation describes our data well, we suggest that irradiance is a
254 major factor influencing the fractionation factor α between the alkenones and growth
255 water of the haptophytes grown in our culture experiments.

256 Schouten et al. (2006) showed that α decreases with increasing growth rate (Fig. 3)
257 potentially suggesting that our observed correlation may be due to changing growth

258 rates controlled by the level of irradiance. However, plotting the growth rate against the
259 fractionation factor α for all irradiances from both experiments performed here shows
260 no clear correlation between α and growth rate (Fig. 3). Fractionation factor α increases
261 from growth rates of 0.4 to approximately 1.2 d⁻¹ after which it decreases a little,
262 although there is some scatter at these higher growth rates. These results suggest that in
263 our experiments α does not change because of changing growth rates, but that both α
264 and growth rate are a function of irradiance. These findings are different from the
265 results of Schouten et al. (2006; Fig. 3), where *E. huxleyi* was grown at constant
266 irradiance but different salinities and temperatures, suggesting that hydrogen isotope
267 fractionation in alkenone biosynthesis in these experiments is more likely controlled by
268 downstream biosynthetic effects.

269 A possible explanation for this effect of irradiance on the hydrogen isotopic
270 fractionation of *E. huxleyi* could be the central role NADPH has as hydrogen source for
271 biosynthesis (Yakir and DeNiro, 1990; Hayes, 2001), i.e. approximately 50% of non-
272 exchangeable hydrogen in lipids is derived from NADPH (Zhang et al., 2009). The
273 initial biosynthetic isotopic fractionation effect from water to the primary photosynthate
274 is considerable, ca. 171 ‰, suggested to be largely due to the reduction of NADP⁺ to
275 NADPH (Yakir and DeNiro, 1990; reviewed by Hayes, 2001). The reduction of
276 NADP⁺ to NADPH in photosynthetic organisms is directly linked to photosystem
277 activity (Allen 2002 and references therein) and therefore potentially light intensity.
278 This probably explains the link between irradiance level and hydrogen isotopic
279 fractionation, although the exact biochemical mechanisms responsible for this irradiance
280 depended hydrogen isotope fractionation effect is unclear and subject for future
281 research.

282

283 *4.2 Potential implications for the natural environment.*

284 The magnitude of the change in $\delta D_{\text{alkenones}}$ between cultures grown at 15 and 200
285 $\mu\text{mol photons m}^{-2} \text{s}^{-1}$ ($\sim 40 \text{‰}$ or 0.2‰ per $\mu\text{mol photons m}^{-2} \text{s}^{-1}$) is relatively large and
286 comparable in magnitude to the change observed for cultures grown in salinities varying
287 by ~ 20 salinity units (i.e. $1\text{-}3 \text{‰}$ change per salinity unit observed in cultures; Schouten
288 et al., 2006; M'Boule et al., 2014; Chivall et al., 2014). This suggests that an irradiance
289 effect could be large enough to limit the applicability of $\delta D_{\text{alkenones}}$ as a proxy for paleo
290 salinity. An important constraint will be the overall *in situ* irradiance level during
291 biomass formation and alkenone synthesis (Wolhowe et al., 2015), as well as how much
292 variability in irradiance, which is related to seasonal variability and water depth, is
293 captured by sedimentary alkenones, especially when averaged over geological time
294 scales.

295 Depending on season, latitude and depth, photosynthetically available radiation in
296 the ocean will range from 0 to approximately $810 \mu\text{mol photons m}^{-2} \text{s}^{-1}$ (Frouin and
297 Murakami 2007), a range almost entirely covered by our irradiance experiments. Our
298 results show that irradiance has the strongest effect on the hydrogen isotopic
299 fractionation at light intensities from 15 to $200 \mu\text{mol photons m}^{-2} \text{s}^{-1}$. This irradiance
300 effect is in agreement with $\alpha_{\text{alkenones/water}}$ in suspended particulate matter from the photic
301 zone of the Gulf of California and the eastern tropical North Pacific which show
302 decreasing values with increasing depth and thus decreasing light levels (Wolhowe et
303 al., 2015).

304 Algae, including alkenone producing haptophytes, tend to form large blooms when
305 the growth conditions, specifically nutrient levels, temperature and irradiance, are

306 optimal. *E. huxleyi*, for instance, is thought to thrive under high light conditions, at
307 mixed layer depths generally <30 meter (Tyrrell and Merico, 2004; Harris et al., 2005).
308 They outcompete other algal species that suffer from photoinhibition under these
309 conditions, a process that is apparently absent in *E. huxleyi* (Nanninga and Tyrrell,
310 1996). In fact, based on field data collected during *E. huxleyi* blooms, mesocosm studies
311 and culture experiments, *E. huxleyi* is thought to only form large blooms at light
312 intensities $>530 \mu\text{mol photons m}^{-2} \text{ s}^{-1}$ (Nanninga and Tyrrell, 1996 and references
313 therein; Harris et al., 2005). This is in the range of irradiance levels in our experiments
314 where α is relatively constant (Fig. 2), indicating that the δD of alkenones synthesized
315 during blooming would show only minor variation due to variations in the level of
316 irradiance. If the majority of alkenones in the sediment are derived from haptophytes
317 blooming at the surface, this indicates that variations in the level of irradiance would
318 only have a minor effect on the δD of sedimentary alkenones. Indeed, it has been
319 shown often that the degree of unsaturation of alkenones, the $U^{K'}_{37}$, which is used as a
320 paleo sea surface temperature proxy, correlates on a global scale best with annual mean
321 sea surface temperatures rather than deeper water temperatures, i.e. at the bottom of the
322 photic zone (e.g. Müller et al., 1998). Furthermore, during bloom conditions when
323 growth becomes limited by nutrient limitation, but photosynthesis continues as long as
324 there is enough light, the haptophyte algae produce more alkenones per cell to store the
325 reducing equivalents (i.e. NADPH) produced during photosynthesis (Eltgroth et al.,
326 2005). High cell densities during bloom conditions might also promote grazing and
327 packaging of cells and alkenones in fecal pellets, cell aggregation and increase the
328 possibility of cell material attaching to sinking particles, increasing the transport
329 efficiency of haptophyte cell material, including alkenones, to the underlying sediment.

330 Therefore it seems likely that the majority of alkenones in the sediment are derived from
331 haptophyte blooms and reflect high light conditions.

332 Nevertheless, the conditions under which the majority of the sedimentary alkenones
333 are produced together with the environmental significance of irradiance on the hydrogen
334 isotope fractionation should be further tested in nature by sampling suspended
335 particulate matter from different water depths (c.f. Wolhowe et al., 2015) and bloom
336 and non-bloom derived alkenones using sediment traps and analyzing core tops from
337 close to the equator to high latitudes to capture seasonal variability in irradiance.

338

339 **5. Conclusion**

340 Cultivation of two *E. huxleyi* strains show that when growth rate is irradiance-
341 limited, increasing growth results in decreased hydrogen isotope fractionation, the
342 opposite response to temperature/salinity-limited growth rate. Rather, our results
343 suggest that irradiance is directly affecting the hydrogen isotopic fractionation of *E.*
344 *huxleyi* up to levels of 200 $\mu\text{mol photons m}^{-2} \text{s}^{-1}$ after which it remains relatively
345 constant. *E. huxleyi* usually thrives under relatively high light conditions and is thought
346 to bloom at light intensities $> 500 \mu\text{mol photons m}^{-2} \text{s}^{-1}$. Therefore, it seems unlikely
347 that light affects the use of the hydrogen isotopic composition of sedimentary long chain
348 alkenones as a proxy for paleosalinity, assuming that the majority of sedimentary
349 alkenones are derived from surface water haptophyte blooms. The actual conditions
350 under which most of the sedimentary alkenones are produced, together with the
351 significance of irradiance on the hydrogen isotopic composition of long chain alkenones
352 in natural settings should be further investigated.

353

354 **6. Acknowledgements**

355 We would like to thank the associate editor, Dr. Canuel, and Dr. Sessions , Dr.
356 Wolhowe and two anonymous reviewers for their constructive comments. This work
357 was supported by the Dutch Organization for Scientific Research (NWO) through a
358 VIDI grant to Marcel van der Meer. A Fulbright research grant was awarded to
359 Katherine French to work at the AWI. Part of this work was funded by the European
360 Science Foundation (ESF) under the EUROCORES Programme “EuroCLIMATE”,
361 through contract No. ERAS-CT-2003-980409 of the European Commission, DG
362 Research, FP6. NWO is also acknowledged for supporting the Dutch part of this
363 program. This work was carried out under the program of the Netherlands Earth System
364 Science Centre (NESSC).

365

366 **7. References**

367 Allen J. F. (2002) Photosynthesis of ATP-electrons, proton pumps, rotors and poise.
368 *Cell* **110**, 273-276.

369 Benthien A., Schulte S., Müller P. J., Schneider R. and Wefer G. (2002) Carbon isotopic
370 composition of the C_{37:2} alkenone in core top sediments of the South Atlantic Ocean:
371 Effects of CO₂ and nutrient concentrations. *Global Biogeochem. Cycles* **16** 1012,
372 10.1029/2001GB001433.

373 Chivall D., M'Boule D., Sinke-Schoen D., Sinninghe Damsté J.S., Schouten S. and van
374 der Meer M. T. J. (2014) The effects of growth phase and salinity on the hydrogen
375 isotopic composition of alkenones produced by coastal haptophyte algae. *Geochim.*
376 *Cosmochim. Acta* **140**, 381-390.

377 Coolen M. J. L., Orsi W. D., Balkema C., Quince C., Harris K., Sylva S. P., Filipova-
378 Marinova M. and Giosan L. (2013) Evolution of the plankton paleome in the Black
379 Sea from the Deglacial to Anthropocene. *Proc. Natl. Acad. Sci. U.S.A.* **110**, 8609-
380 8614.

381 Craig H. and Gordon L.I. (1965) Deuterium and oxygen 18 variations in the ocean and
382 marine atmosphere, Proceedings of a Conference on Stable Isotopes in
383 Oceanographic Studies and Paleotemperatures. Pisa: V. Lischi & Figli., Spoleto,
384 Italy, pp. 9 - 130.

385 Eilers P. H. C. and Peeters J. C. H. (1988) A model for the relationship between light
386 intensity and the rate of photosynthesis in phytoplankton. *Ecol. Model.* **42**, 199-215.

387 Eltgroth M. L., Watwood R. L., Wolfe G. V. (2005) Production and cellular localization
388 of neutral long-chain lipids in the haptophyte algae *Isochrysis galbana* and *Emiliania*
389 *Huxleyi*. *J. Phycol.* **41**, 1000-1009.

390 Englebrecht A. C. and Sachs J. P. (2005) Determination of sediment provenance at drift
391 sites using hydrogen isotopes and unsaturation ratios in alkenones. *Geochim.*
392 *Cosmochim. Acta* **69**, 4253-4265.

393 Giosan L., Coolen M. J. L., Kaplan J. O., Constantinescu S., Filip F., Filipova-Marinova
394 M., Kettner A. J. and Thom N. (2012) Early anthropogenic transformation of the
395 Danube-Black Sea system. *Scientific reports* **2**:582.

396 Guillard R. R. L. (1975) Culture of phytoplankton for feeding marine invertebrates. In
397 *Culture of Marine Invertebrate Animals* (eds. W. L. Smith and M. H. Chanley).
398 Plenum Press, New York. pp. 26-60.

399 Feng Y., Warner M. E., Zhang Y., Sun J., Fu F.-X., Rose J. M. and Hutchins D. A.
400 (2008) Interactive effects of increased pCO₂, temperature and irradiance on the

401 marine coccolithophore *Emiliana huxleyi* (Prymnesiophyceae). *Eur. J. Phycol.* **43**,
402 87-98.

403 Flameling I. A. and Kromkamp J. (1998) Light dependence of quantum yields for PSII
404 charge separation and oxygen evolution in eucaryotic algae. *Limnol. Oceanogr.* **43**,
405 284-297.

406 Frouin R. and Murakami H. (2007) Estimating Photosynthetically Available Radiation
407 at the Ocean Surface from ADEOS-II Global Imager Data. *J Oceanography* **63**,
408 493-503.

409 Harris G. N., Scanlan D. J. and Geider R. J. (2005) Acclimation of *Emiliana huxleyi*
410 (Prymnesiophyceae) to photon flux density. *J. Phycol.* **41**, 851-862.

411 Hayes J. M. (2001) Fractionation of the isotopes Carbon and Hydrogen in biosynthetic
412 processes. In *Stable Isotope Geochemistry*. The Mineralogical Society of America,
413 Washington. pp. 225–277.

414 Kasper S., van der Meer M. T. J., Mets A., Zahn R., Sinninghe Damsté J. S., and
415 Schouten S. (2014) Salinity changes in the Agulhas leakage area recorded by stable
416 hydrogen isotopes of C₃₇ alkenones during Termination I and II, *Clim. Past* **10**, 251-
417 260.

418 Kasper S., van der Meer M. T. J., Castañeda I. S., Tjallingii R., Brummer G.-J.,
419 Sinninghe Damsté J. S., and Schouten S. (2015) Testing the alkenone D/H ratio as a
420 paleo indicator of sea surface salinity in a coastal ocean margin (Mozambique
421 channel). *Org. Geochem.* **78**, 62-68.

422 Langer G., Nehrke G., Probert I., Ly J. and Ziveri P. (2009) Strain-specific responses of
423 *Emiliana huxleyi* to changing seawater carbonate chemistry. *Biogeosciences* **6**,
424 2637-2646.

425 Marino G., Rohling E. J., Rijpstra W. I. C., Sangiorgi F., Schouten S., and Sinninghe
426 Damsté J. S. (2007) Aegean Sea as driver of hydrographic and ecological changes in
427 the eastern Mediterranean. *Geology* **35**, 675-678.

428 Marlowe I. T., Green J. C., Neal A. C., Brassell S. C., Eglinton G. and Course P. A.
429 (1984) Long-chain (*n*-C37-C39) alkenones in the Prymnesiophyceae. Distribution of
430 alkenones and other lipids and their taxonomic significance. *Brit. Phycol. J.* **19**, 203-
431 216.

432 M'Boule D., Chivall D., Sinke-Schoen D., Sinninghe Damsté J. S., Schouten S. and van
433 der Meer, M. T. J. (2014) Salinity dependent hydrogen isotope fractionation in
434 alkenones produced by open ocean and coastal haptophyte algae. *Geochim.*
435 *Cosmochim. Acta* **130**: 126-135.

436 Müller P. J., Kirst G., Ruhland G., von Storch I., Rosell-Melé A. (1998) Calibration of
437 the alkenone paleotemperature index $U_{37}^{K'}$ based on core-tops from the eastern
438 South Atlantic and the global ocean (60°N-60°S). *Geochim. Cosmochim. Acta* **62**,
439 1757-1772.

440 Nanninga H. J. and Tyrrell T. (1996) Importance of light for formation of algal blooms
441 by *Emiliana huxleyi*. *Mar. Ecol. Prog. Ser.* **136**, 195-203.

442 Nelson D. B. and Sachs J. P. (2014) The influence of salinity on D/H fractionation in
443 alkenones from saline and hypersaline lakes in continental North America. *Org.*
444 *Geochem.* **66**, 38-47.

445 Nelson D. B. and Sachs J. P. (2014) The influence of salinity on D/H fractionation in
446 dinosterol and brassicasterol from globally distributed saline and hypersaline lakes.
447 *Geochim. Cosmochim. Acta* **133**, 325-339.

448 Paul H. A. (2002) Application of novel stable isotope methods to reconstruct
449 paleoenvironments. Ph. D. thesis, Swiss Federal Institute of Technology, Zürich.

450 Sachs J. P. and Schwab V. F. (2011) Hydrogen isotopes in dinosterol from the
451 Chesapeake Bay estuary. *Geochim. Cosmochim. Acta* **75**, 444-459.

452 Sachse D. and Sachs J. P. (2008) Inverse relationship between D/H fractionation in
453 cyanobacterial lipids and salinity in Christmas Island saline ponds. *Geochim.*
454 *Cosmochim. Acta* **72**, 793-806.

455 Schouten S., Ossebaar J., Schreiber K., Kienhuis M. V. M., Langer G., Benthien A., and
456 Bijma J. (2006) The effect of temperature, salinity and growth rate on the stable
457 hydrogen isotopic composition of long chain alkenones produced by *Emiliana*
458 *huxleyi* and *Gephyrocapsa oceanica*. *Biogeosciences* **3**, 113-119.

459 Schwab V. F. and Sachs J. P. (2011) Hydrogen isotopes in individual alkenones from
460 the Chesapeake Bay estuary. *Geochim. Cosmochim. Acta* **75**, 7552-7565.

461 Sessions A.L., Sylva S.P., Summons R.E., Hayes J.M. (2004) Isotopic exchange of
462 carbon-bound hydrogen over geologic timescales. *Geochim. Cosmochim. Acta* **68**,
463 1545-1559.

464 Soetaert K., Herman P. M. J. and Kromkamp J. (1994) Living in the twilight: estimating
465 net phytoplankton growth in the Westerschelde estuary (The Netherlands) by means
466 of an ecosystem model (MOSES). *J. Plankton Res.* **16**, 1277-1301.

467 Tyrrell T. and Merico A. (2004) *Emiliana huxleyi*: bloom observations and the
468 conditions that induce them. In *Coccolithophores: From Molecular Processes to*
469 *Global Impact* (eds. H.R. Thierstein and J.R. Young). Springer Science, Dordrecht,
470 The Netherlands. pp 75-97.

471 van der Meer M. T. J., Baas M., Rijpstra W. I. C., Marino G., Rohling E. J., Sinninghe
472 Damsté J. S., and Schouten S. (2007) Hydrogen isotopic compositions of long-chain
473 alkenones record freshwater flooding of the Eastern Mediterranean at the onset of
474 sapropel deposition. *Earth. Planet. Sci. Lett.* **262**, 594-600.

475 van der Meer M. T. J., Sangiorgi F., Baas M., Brinkhuis H., Sinninghe Damsté J. S., and
476 Schouten S. (2008) Molecular isotopic and dinoflagellate evidence for Late
477 Holocene freshening of the Black Sea. *Earth. Planet. Sci. Lett.* **267**, 426-434.

478 van der Meer M. T. J., Benthien A., Bijma J., Schouten S. and Damsté J. S. S. (2013)
479 Alkenone distribution impacts the hydrogen isotopic composition of the C_{37:2} and
480 C_{37:3} alkan-2-ones in *Emiliana huxleyi*. *Geochim. Cosmochim. Acta* **111**, 162-166

481 Volkman J. K., Eglinton G., Corner E. D. S. and Sargent J. R. (1980) Novel unsaturated
482 straight-chain C₃₇–C₃₉ methyl and ethyl ketones in marine sediments and a
483 coccolithophore *Emiliana huxleyi*. In *Advances in Organic Geochemistry, 1979*
484 (eds. A. G. Douglas and J. R. Maxwell). Pergamon Press, Oxford. pp. 219-227.

485 Volkman J. K., Barrett S. M., Blackburn S. I. and Sikes E. L. (1995) Alkenones in
486 *Gephyrocapsa oceanica*: Implications for studies of paleoclimate. *Geochim.*
487 *Cosmochim. Acta* **59**, 513-520.

488 Wolhowe M. D., Prahl F. G., Probert I., and Maldonado M. (2009) Growth phase
489 dependent hydrogen isotopic fractionation in alkenone-producing haptophytes.
490 *Biogeosciences* **6**, 1681-1694.

491 Wolhowe M. D., Prahl F. G., Desiderio R. A., Langer G., Oviedo A. M. and Ziveri P.
492 (2015) Alkenone δD as an ecological indicator: A culture, model, and field study of
493 physiologically-controlled chemical and hydrogen-isotopic variation in C₃₇
494 alkenones. *Geochim. Cosmochim. Acta Accepted*.

495 Wong W. W. and Clarke L. L. (2012) A hydrogen gas-water equilibrium method
496 produces accurate and precise stable hydrogen isotope ratio measurements in
497 nutrition studies. *J. Nutr.* **142**: 2057-2062.

498 Yakir D. and DeNiro M. J. (1990) Oxygen and hydrogen isotope fractionation during
499 cellulose metabolism in *Lemna gibba* L. *Plant physiol.* **93**, 325–32.

500 Zhang X., Gillespie A.L. and Sessions A. (2009) Large D/H variations in bacterial lipids
501 reflect central metabolic pathways. *Proc. Natl. Acad. Sci. U.S.A.* **106**: 12580-12586.

502

503 **Figure legends**

504 Figure 1: Growth rate μ (d^{-1}) plotted against irradiance I ($\mu\text{mol photons m}^{-2} \text{s}^{-1}$) for both
505 the first experiment with *E. huxleyi* strain PML B92/11 (●) and second experiment
506 with strain RCC1238 (▲) and the model fit using the Eilers-Peeters equation (Eq.
507 1) (---)(Eilers and Peeters, 1988) .

508 Figure 2: Fractionation factor α alkenones versus medium water plotted against
509 irradiance I ($\mu\text{mol photons m}^{-2} \text{s}^{-1}$) for both the first experiment with *E. huxleyi*
510 strain PML B92/11 (●) and second experiment with strain RCC1238 (▲) and the
511 model fit using a modified Eilers-Peeters equation (Eq. 2) (---)(Eilers and Peeters,
512 1988).

513 Figure 3: Fractionation factor α for alkenones versus medium water plotted against
514 growth rate μ (d^{-1}) for both the first with *E. huxleyi* strain PML B92/11 (●) and
515 second experiment with strain RCC1238 (▲) in which both α and μ were
516 controlled by light intensity. Included are also the α and μ data from Schouten et
517 al., 2006 (×) for *E. huxleyi* grown at different salinities and temperatures at a single
518 light intensity.

519 **Table 1:** Results from two culture experiments in which two strains of *E. huxleyi* (PML
520 B92/11 and RCC1238) were cultured at different light intensities to study the effect of
521 light intensity on hydrogen isotope fractionation. All cultures were harvested in the
522 exponential growth phase after 4 to 12 days depending on the cell numbers.
523

Irradiance <i>I</i> ($\mu\text{mol photons m}^{-2} \text{s}^{-1}$)	Growth rate μ (d^{-1})	$\delta\text{D}_{\text{water}}$ (‰ vs. VSMOW)	Stdev	$\delta\text{D}_{\text{alkenones}}$ (‰ vs. VSMOW)	Stdev	α	Error
<i>Experiment 1</i>							
<i>Strain PML</i>							
<i>B92/11</i>							
15	0.47	-1.5	2.5	-233.2	3.2	0.768	0.004
15	0.48	-2.9	2.2	-229.3	0.1	0.773	0.002
30	0.76	-0.7	1.5	-231.4	0.1	0.769	0.001
30	0.87	-2.0	2.3	-231.8	2.2	0.770	0.003
50	0.94	-1.1	1.8	-231.6	2.3	0.769	0.003
50	0.95	-0.7	1.4	-218.6	2.3	0.782	0.003
100	1.02	-1.7	1.7	-209.2	0.8	0.792	0.002
100	1.13	-1.3	2.0	-209.5	0.8	0.792	0.002
100	1.08	-2.3	1.3	-209.9	1.5	0.792	0.002
200	1.05	-2.0	1.4	-186.8	2.4	0.815	0.003
200	1.14	-0.9	1.8	-191.1	1.8	0.810	0.002
<i>Experiment 2</i>							
<i>Strain</i>							
<i>RCC1238</i>							
100	1.26	-0.3	1.3	-213.6	2.1	0.787	0.002
100	1.30	0.2	1.6	-214.8	1.1	0.785	0.002
100	1.28	-1.1	2.1	-209.8	1.8	0.791	0.002
200	1.24	-2.4	1.9	-186.3	1.0	0.816	0.002
200	1.25	-0.7	0.0	-189.8	1.1	0.811	0.001
200	1.24	-1.8	2.6	-187.1	2.0	0.814	0.003
400	1.24	1.2	1.3	-192.9	5.0	0.806	0.005
400	1.27	0.4	1.2	-192.3	0.5	0.807	0.001
400	1.24	0.3	1.2	-188.5	5.4	0.811	0.006
600	1.30	-2.8	1.5	-196.8	2.7	0.805	0.003
600	1.32	-0.9	0.2	-196.4	2.9	0.804	0.003
600	1.31	0.1	4.8	-192.6	3.1	0.807	0.005

524
525

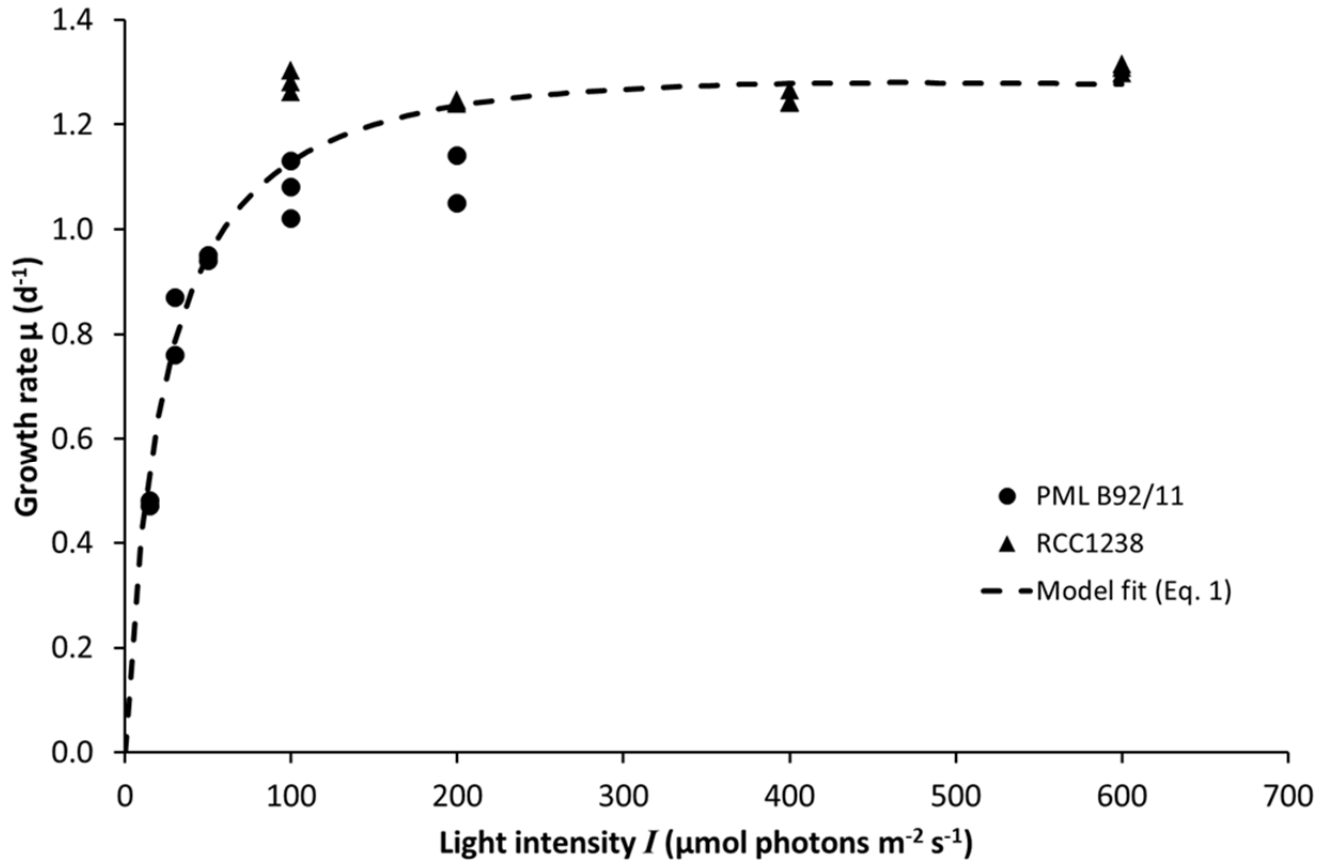


Figure 1

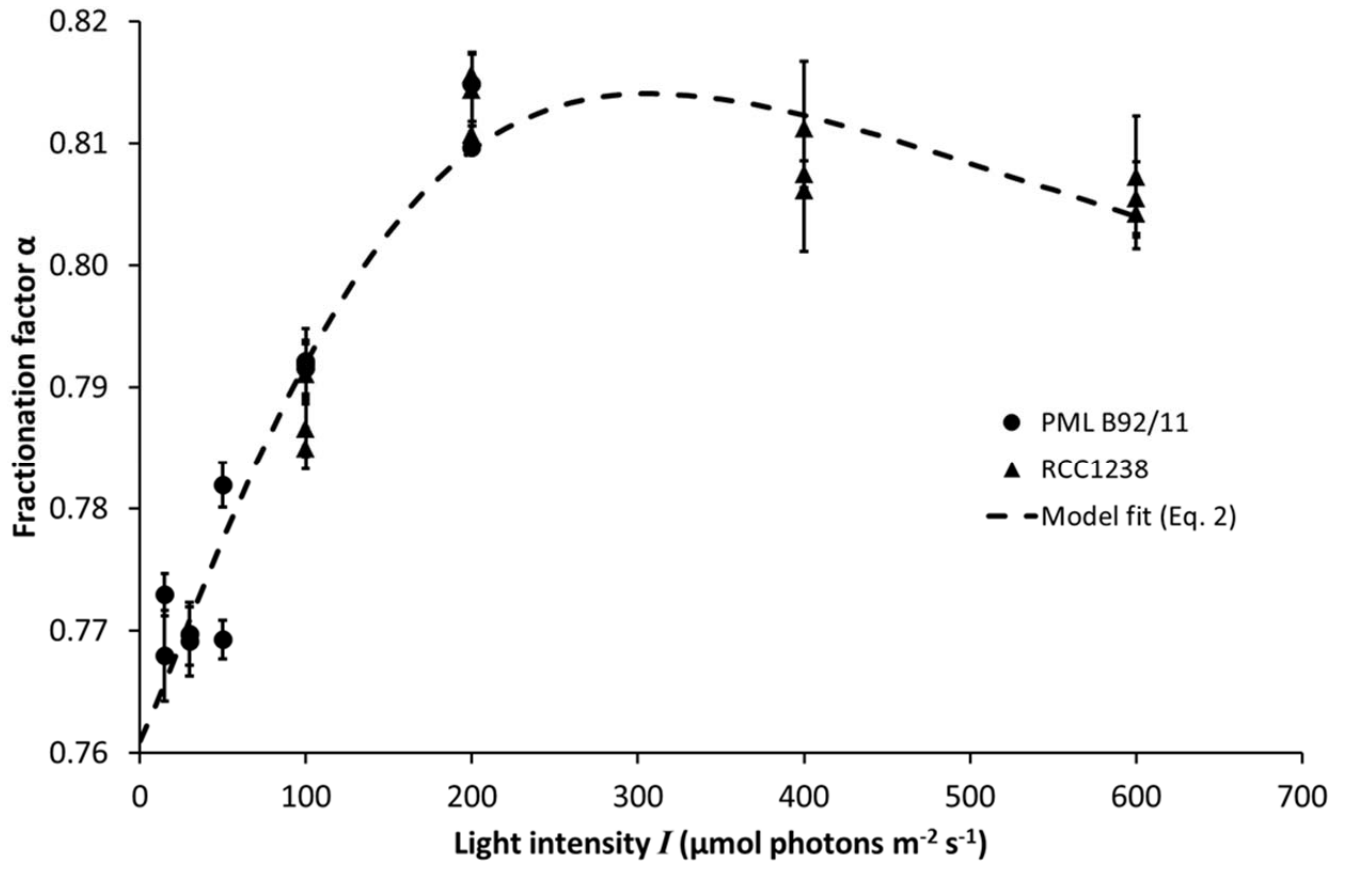


Figure 2

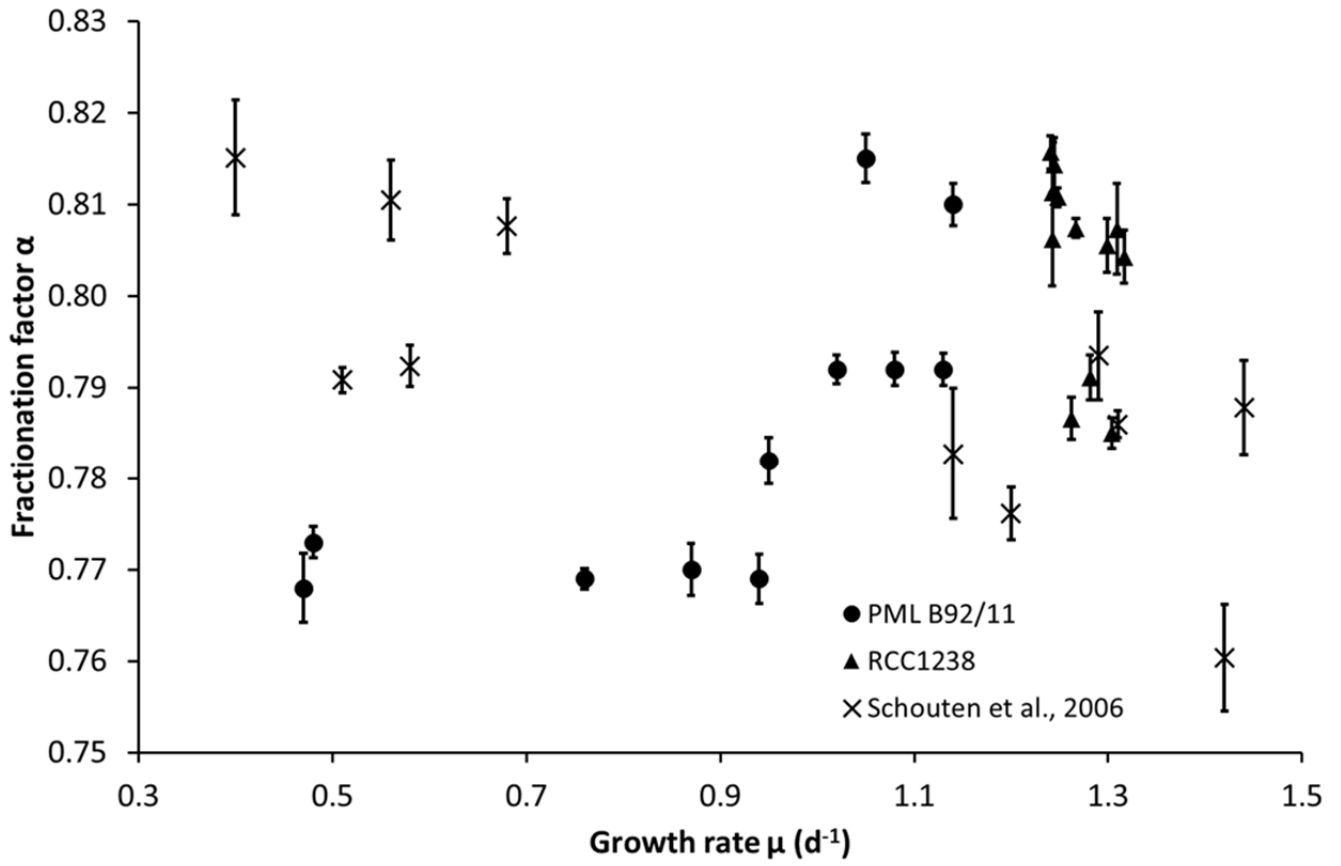


Figure 3